Skeletal Radiology (2018) 47:579–585
https://doi.org/10.1007/s00256-017-2818-z

CASE REPORT

Parosteal extra-axial chordoma of the second metacarpal bone: a case report with literature review

Shinji Tsukamoto[1] · Daniel Vanel[2] · Alberto Righi[2] · Davide Maria Donati[1] · Costantino Errani[1]

Received: 14 December 2016 / Revised: 20 September 2017 / Accepted: 31 October 2017 / Published online: 18 November 2017

Abstract
Extra-axial chordoma is a chordoma that occurs in non-axial locations. It is a very rare tumor, with 20 cases reported to date; 14 in bone and six in soft tissue. Of the 14 skeletal extra-axial chordomas, ten were intramedullary and four were intracortical. We report the first case of parosteal extra-axial chordoma arising in the second metacarpal bone, expressing brachyury on immunohistochemical analysis, and describe the pathologic and radiologic findings. We suggest that extra-axial chordoma can occur in parosteal bone lesions or the hand, without features of bone distribution or bone-specific sites.

Keywords Chordoma · Parachordoma · Extra-axial chordoma · Brachyury · Metacarpal bone · Parosteal

Introduction

Chordoma is a low-grade, slow-growing, malignant bone tumor. The vast majority of chordomas arise as a sporadic disease [1]. There is some evidence that chordoma can develop from a benign notochordal cell tumor [1, 2]. Thirty-seven percent or fewer patients develop metastases, and these usually develop late [3]. The overall median survival time is 6.29 years [2]. Chordoma is a chemo- and radio-resistant tumor, and resection is the first choice of treatment. Recently, carbon ion therapy has been suggested as a treatment option for unresectable sacral chordomas [4].

Extra-axial chordoma is a chordoma that arises in the extra-axial skeleton. Twenty cases of extra-axial chordoma expressing brachyury have been reported to date: 14 in bone and six in soft tissues (Table 1) [2, 5–13]. Brachyury, a transcription factor involved in posterior mesoderm formation and axial development, is a highly specific marker for chordoma and extra-axial chordoma [2], and its expression is necessary for diagnosis of these tumors [5]. Before the diagnostic effectiveness of brachyury was reported, extra-axial chordoma was diagnosed as parachordoma [5]. Currently, brachyury-negative parachordoma is diagnosed as a spectrum of mixed tumor/myoepithelioma/parachordoma [5]. Of these skeletal extra-axial chordomas, ten were intramedullary and four were intracortical [2, 6–9, 11–13]. We report the first case of parosteal extra-axial chordoma of the metacarpal bone, and describe the radiologic and pathologic findings.

Case report

A 20-year-old man with no previous history of major illness presented with a 10-month history of pain and swelling around the left second metacarpophalangeal joint. Routine laboratory data were normal. Radiographs revealed a lytic lesion of the distal epiphysis of the second metacarpal bone, with cortical thickening of the shaft (Fig. 1). On 1.5-T magnetic resonance imaging (Signa Infinity, General Electric, Fairfield, CT, USA) a round lesion abutting on the cortex was observed; it had a low signal intensity on T1 W images (Fig. 2a), high signal intensity on T2 W images (Fig. 2b) and intense enhancement after intravenous contrast (DOTAREM, Guerbet, Roissy, France)(Fig. 2c). A perilesional edema was visible on fat-suppressed T1 W images after contrast injection (Fig. 2c) and fat-suppressed T2 W images (Fig. 2d). The radiological differential diagnosis included a periosteal chondroma or chondrosarcoma, an osteoid osteoma, a periosteal osteoblastoma, an eosinophilic granuloma, and osteomyelitis. Because perilesional edema is uncommon in periosteal chondroma [14], occurrence of this was considered unlikely in

✉ Daniel Vanel
daniel.vanel@ior.it

[1] Department of Orthopaedic Oncology, Rizzoli Institute, Bologna, Italy

[2] Department of Pathology, Rizzoli Institute, Via di Barbiano 1/10, 40136 Bologna, Italy

Table 1 Literature review of extra-axial chordomas

Sr no.	Author (year)	Age/gender	Site	Location	Perilesional edema	Brachyury expression	Treatment	Outcome
1	Nielsen et al. (2001) [6]	36/M	Distal ulna	Intra-medullary (central)	−	+	Resection	CDF (30 months)
2	Van Akkooii et al. (2006) [7]	56/F	10th rib	Intra-medullary (eccentric)	NA	+	Resection	CDF (4 months)
3	Di Francesco et al. (2006) [8]	41/F	Pubis	Intra-medullary (NA)	NA	+	Resection +50 cGy-EBRT	CDF (84 months)
4	O'Donnell et al. (2007) [9]	27/M	Proximal tibia	Intracortical	+	+	Excision + bone grafting	CDF (36 months)
5	Tirabosco et al. (2008) [1]	35/M	Mid tibia	Intracortical	NA	+	Resection	CDF (18 months)
		55/F	1st metatarsal	Intra-medullary (eccentric)	NA	+	Resection	CDF (54 months)
		68/M	Distal femur	Intra-medullary (NA)	NA	+	Resection	AWD (40 months)
		18/F	Proximal tibia	Intra-medullary (eccentric)	+	+	Curettage	AWD (14 months)
		66/M	Dorsum thumb	Juxta-articular		+	Resection	CDF (161 months)
		44/M	Wrist	Juxta-articular		+	Resection	LFU
		55/M	Gluteus maximus	Intra-muscular		+	Resection	CDF (5 months)
		50/F	Para vertebral	Deep soft tissue		+	Resection	LFU
6	De Comas et al. (2010) [10]	28/M	Shoulder	Intra-muscular		+	Resection	CDF (24 months)
7	Suzuki et al. (2011) [5]	87/M	Wrist	Juxta-articular		+	Resection	CDF (32 months)
8	Lantos et al. (2013) [11]	21/F	Distal femur	Intracortical	+	+	Excision + bone grafting	AWD (24 months)
		21/F	Distal tibia	Intracortical	+	+	Curettage, excision	CDF (36 months)
9	Rekhi (2015) [12]	42/M	Proximal tibia	Intra-medullary (eccentric)	NA	+	Curettage + bone grafting	CDF (3 months)
10	Evans et al. (2016) [13]	68/M	Distal femur	Intra-medullary (NA)	NA	+	Resection	DOD (26 months)
		36/M	Distal ulnar	Intra-medullary (central)	−	+	Resection	CDF (130 months)
		59/M	Proximal fibula	Intra-medullary (central)	−	+	Resection	CDF (26 months)

Sr series, *EBRT* external beam radiotherapy, *CDF* continuous disease free, *AWD* alive with disease (local recurrence), *LFU* lost at follow-up, *DOD* death of disease, *NA* not available

Fig. 1 Radiograph showing poorly visible lytic lesion of the distal epiphysis of the second metacarpal bone (*arrow*). The non-calcified soft tissue component is not visible

our case. Periosteal edema is more frequently seen in periosteal chondrosarcoma; consequently this entity needs to be ruled out in the differential diagnosis [11]. On radiographs, osteoid osteoma is usually characterized by dense cortical sclerosis surrounding a radiolucent nidus [1]; therefore this was also unlikely in our case. Periosteal osteoblastoma is rare, with a radiologic appearance that varies from a lytic lesion with internal calcification to a heavily calcified mass, and with diffuse perilesional edema; therefore, this entity was also part of the differential diagnosis [15]. An eosinophilic granuloma cannot be distinguished from a skeletal extra-axial chordoma using imaging because it can show perilesional edema and mimic an aggressive lesion [16]. Osteomyelitis was less likely in the absence of imaging findings, such as a sequestrum [11]. Based on the above criteria, it seemed unlikely that the lesion was a malignant tumor. We therefore performed an incisional biopsy to carry out the diagnosis before screening the bone and lung. A longitudinal skin incision was made over on the radial side of the second metacarpal bone. White and enlarged synovium-like tissue, located close to the metacarpophalangeal joint, was collected and submitted for pathological examination; no pathogens were cultured from the collected tissue. Histological examination showed a cellular proliferation organized in nests and cords in an abundant extracellular myxoid matrix separated into lobules by fibrous septa. Peritumoral edema was found in the medullary cavity of the bone and in soft tissues. The neoplastic cells had coarse nuclear chromatin and copious vacuolated cytoplasm, referred to as "physaliferous cells" (Fig. 3a). Immunohistochemical analysis confirmed strong staining for brachyury (Fig. 3b), epithelial membrane antigen, and focal immunostaining for pankeratin. Smooth muscle actin, S-100 protein, desmin, p63, calponin, and glial fibrillary acidic protein were negative. Fluorescence in situ hybridization analysis did not reveal rearrangement of the Ewing sarcoma breakpoint region 1. Morphologically, the main pathological differential diagnosis included extra-axial chordoma and myoepithelioma. The strong immunohistochemical expression of brachyury, which is a specific marker of physaliferous cells [1], and the absence of the Ewing sarcoma breakpoint region 1 rearrangement often found in myoepithelioma [17], are essential in diagnosing extra-axial chordoma. F-18 fluorodeoxyglucose (FDG) positron emission tomography (PET)/computed tomography (CT) showed increased FDG uptake in the left second metacarpal bone. Slight linear FDG uptake was seen in the vertebrae (Fig. 4). This was considered a probable artifact, as the high-resolution CT at the same level was normal (Fig. 5). The maximum standardized uptake value of the lesion was 5.1 (Fig. 4). Chest CT showed no lung metastases. Wide resection of the second metacarpal bone was planned. It was impossible to preserve the digital vessels and the extensor and flexor tendons that were adjacent to the tumor. Therefore, ray resection of the finger was performed. A racquet-shaped incision was used from the metacarpophalangeal joint of the index finger to the dorsal side of the second metacarpal bone. The extensor and flexor tendons of the index fingers were transected at the base of the metacarpal bone. Osteotomy of the base of the metacarpal bone was performed. The digital arteries and veins were ligated and cut, and the nerves were isolated and transected. The tumor was removed, including the partial interosseous muscles of the index finger. Macroscopically, the surgical specimen showed an ovular lobulated nodule that was 0.8 cm in diameter, with a smooth flesh-colored surface, attached by a broad base to the underlying cortex of the second metacarpal bone (Fig. 6). The lesion was mushroom-shaped, abutting the cortex of the bone, and trabecular infiltration of the bone was apparent (Fig. 7). The neoplasm was considered as being a parosteal lesion, based on Figs. 6 and 7. A final diagnosis of parosteal extra-axial chordoma of the metacarpal bone was made. At 12-month follow-up, there was no evidence of local recurrence or distant metastases.

Discussion

We report a case of parosteal extra-axial chordoma of the second metacarpal bone. To date, there have been only 20 case reports of extra-axial chordomas in the English literature (Table 1). Ours is the first case of extra-axial chordoma arising in the metacarpal bone. The extra-axial chordoma of metacarpal origin was a parosteal bone lesion, while all other skeletal extra axial origins were cortical or intramedullary (Table 1).

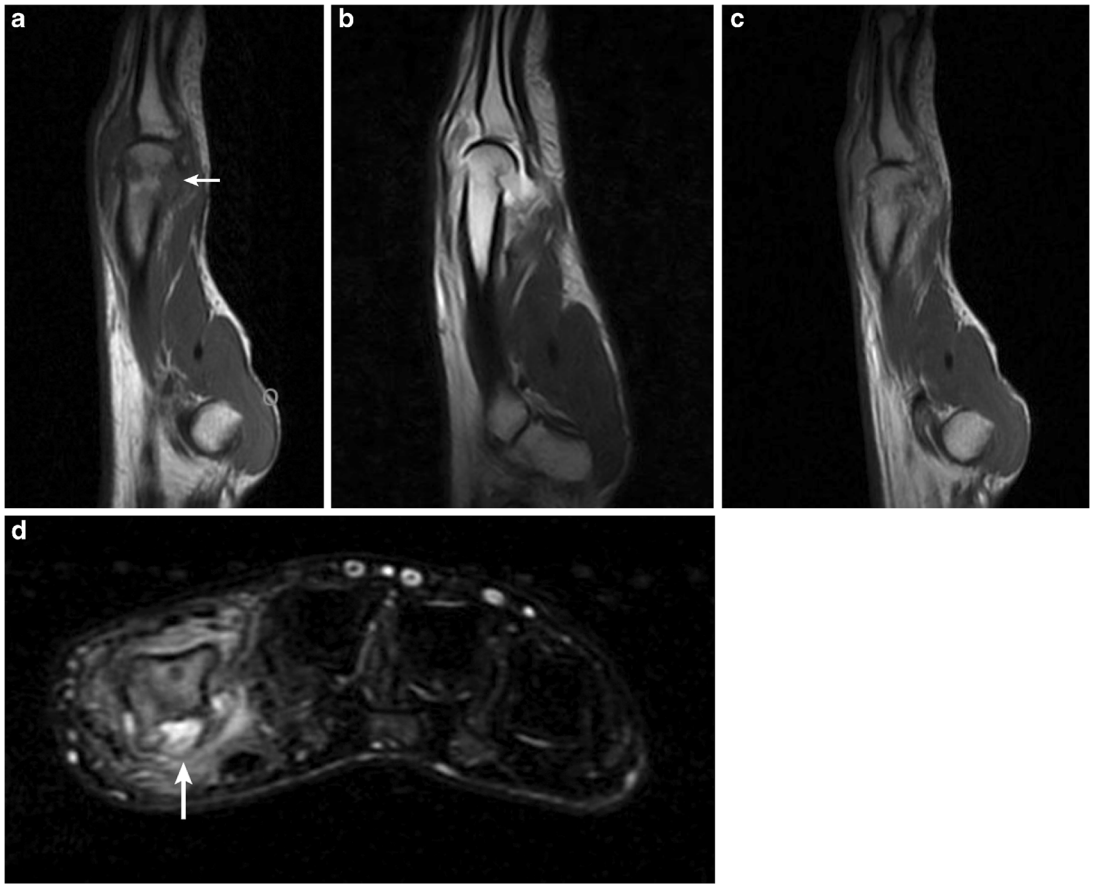

Fig. 2 Magnetic resonance images. **a** Sagittal T1 W (TR/TE = 500/14), **b** T2 W (TR/TE = 2370/80) and **c** after contrast medium injection. The lesion is centered on the eroded cortex, and extends minimally inside the medullary cavity, and more extensively into the soft tissues. It has a low signal on T1 W images (*arrow*) and high signal on T2 W images and after injection. **d** On the axial fat-suppressed T2 W image (TR/TE = 3520/66), the lesion is centered on the cortex (*arrow*), and is surrounded by a poorly limited high signal intensity edema

This study underscores the fact that this unusual tumor is difficult to recognize on imaging, and does not have a predilection for any bone or site within the bone. Extra-axial chordoma seems to be distributed in patients of all ages and in

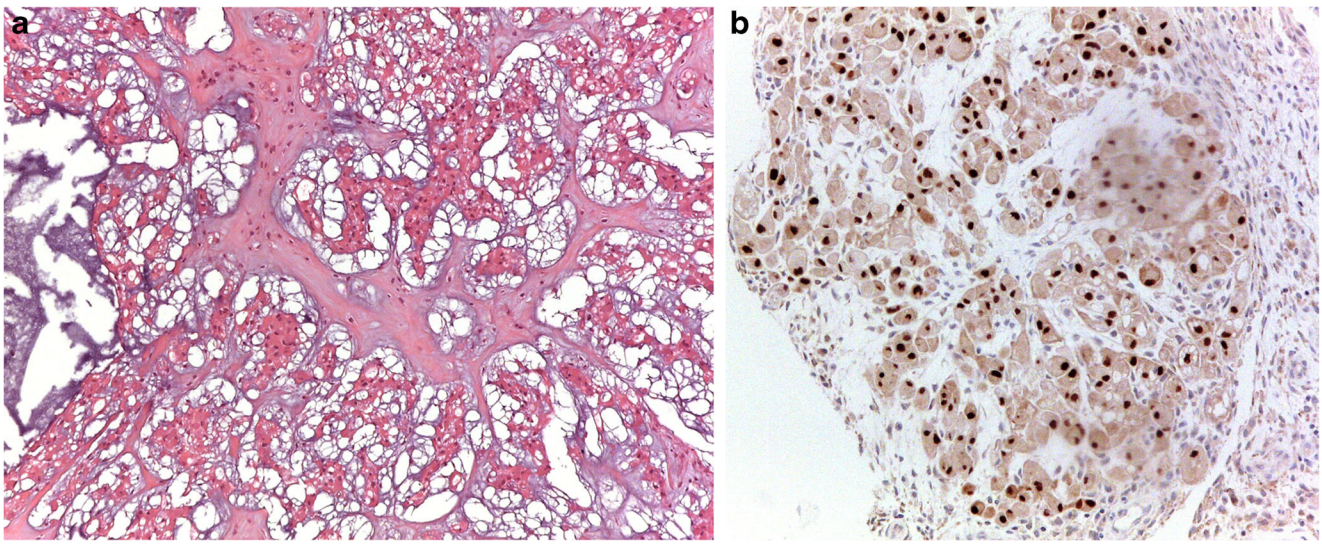

Fig. 3 Photomicrographs of tumor sections. **a** Hematoxylin and eosin-stained section showing the lobulated architecture and extracellular myxoid matrix of the neoplasm composed of large cells with clear to eosinophilic cytoplasms (100× magnification). **b** The nuclei of the neoplasm show a strong immunoreactivity for brachyury (200× magnification) associated with cytoplasmic expression

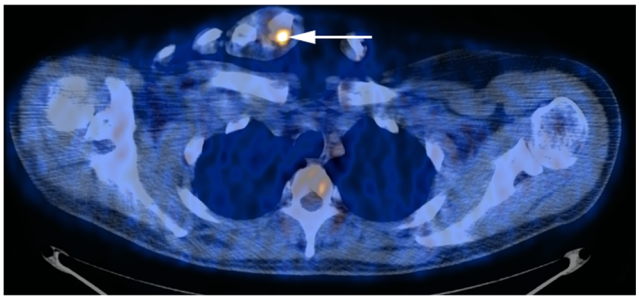

Fig. 4 FDG PET/CT image showing increased FDG uptake in the left second metacarpal bone (*arrow*) and no uptake in other locations. The maximum standardized uptake value of the lesion was 5.1

a wide variety of bones; the tumors are located in the medulla, cortex, subarticular area, metaphysis, and diaphysis (Table 1) [2]. Although axial chordoma commonly develops in the fifth to seventh decades of life [1], extra-axial chordomas can occur earlier [2, 11], as in our case. Extra-axial chordomas seem to behave like their axial counterparts: they are slow-growing tumors and recur if not widely excised [2]. Extra-axial chordomas treated with curettage exhibit local recurrence and one patient is reported to have died because of lung metastases [2, 13].

Our search of the English literature revealed that no case of a periosteal or parosteal bone lesion has been reported [2, 6–9, 11–13]. Here, we report the first case of a parosteal extra-axial skeletal chordoma. As summarized in Table 1, three cases involving an intracortical lesion and one case involving an intramedullary eccentric lesion had perilesional edema [2, 9, 11], while two cases involving an intramedullary central lesion did not [6, 13]. Perilesional edema seems to exist more frequently in intramedullary eccentric, intracortical, and parosteal lesions, as in our case.

F-18 FDG PET/CT usually demonstrates increased uptake of FDG in axial chordoma [18–20]. In our case, F-18 FDG PET/CT showed increased FDG uptake in the left second metacarpal bone and slight FDG uptake, likely due to an artifact in the vertebrae. Because it is difficult to differentiate extra-axial chordoma and metastasis from axial chordoma, PET/CT was useful in confirming the diagnosis of an extra-axial chordoma. Chest CT confirmed that the extra-axial chordoma of the metacarpal bone had not metastasized to the lung.

Fig. 5 High-resolution CT showing no tumor in the thoracic vertebrae with slight FDG uptake

Fig. 6 Photomacrograph of tumor section. The specimen shows an ovular lobulated nodule with a smooth flesh-colored surface extending from the bone into the soft tissue

The lesion in the present case occurred in a metacarpal bone. Primary bone tumors of the small tubular bones of the hand are rare, accounting for 2–5% of all skeletal tumors [21]. Furthermore, the majority of osseous tumors of the hand are benign [22] and most commonly include enchondroma, osteoid osteoma, giant cell tumor, osteochondroma, simple bone cyst, aneurysmal bone cyst, chondromyxoid fibroma, and periosteal chondroma [23–25]. Although primary malignant osseous tumors of the hands are exceedingly rare, reported tumors include chondrosarcoma, osteosarcoma, and Ewing sarcoma [26]. It is challenging to diagnose a bone lesion in the metacarpal bones, because the entire diameter of the bone may be involved, making it difficult to determine from which part of the bone the lesion originated, namely cortical, juxtacortical, or medullary [27]. Our case report suggests the possible existence of this very rare tumor not only outside the spine but also in the hand, an anatomical site usually affected by benign lesions.

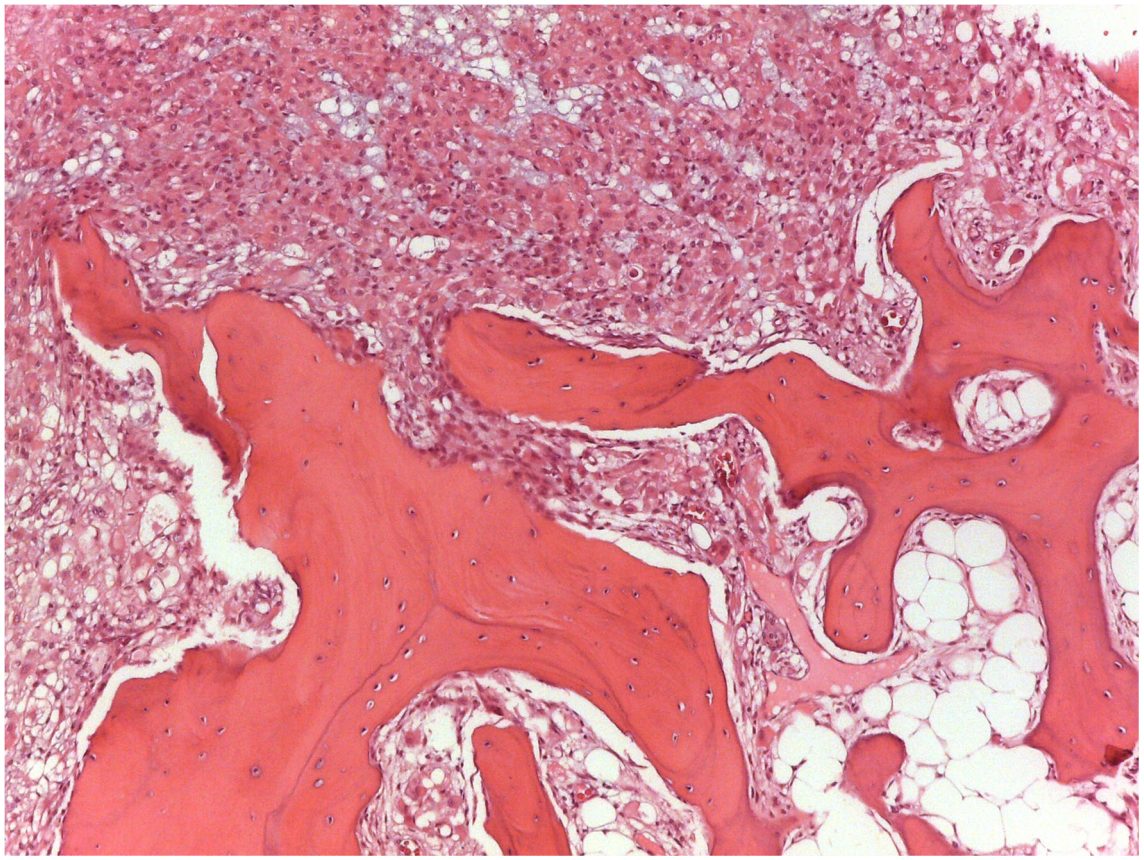

Fig. 7 Photomicrograph of tumor section. Nests and cords of neoplastic cells can be seen infiltrating the trabecular bone (hematoxylin and eosin; 200× magnification)

We suggest that extra-axial chordoma can occur in parosteal bone lesion or the hand, without features of distribution of bone or bone-specific sites. Biopsy is mandatory to obtain a correct diagnosis. An exact diagnosis has therapeutic relevance because this tumor has a relatively favorable outcome when treated with wide resection [12]. It is important to gather case reports in the international literature to better understand prognosis, survival, and tumor recurrence rates following treatment.

Compliance with ethical standards

Conflict of interest The authors declare that they have no conflicts of interest.

Author statement All authors had access to data and a role in writing the manuscript.

References

1. Fletcher CDM, Bridge JA, Hogendoorn P, Mertens F. WHO Classification of Tumours of Soft Tissue and Bone. Lyon: IARC; 2013.
2. Yamaguchi T, Watanabe-Ishiiwa H, Suzuki S, Igarashi Y, Ueda Y. Incipient chordoma: a report of two cases of early-stage chordoma arising from benign notochordal cell tumors. Mod Pathol. 2005;18(7):1005–10.
3. Tirabosco R, Mangham DC, Rosenberg AE, et al. Brachyury expression in extra-axial skeletal and soft tissue chordomas: a marker that distinguishes chordoma from mixed tumor/myoepithelioma/parachordoma in soft tissue. Am J Surg Pathol. 2008;32(4):572–80.
4. Imai R, Kamada T, Tsuji H, Yanagi T, Baba M, Miyamoto T, et al. Carbon ion radiotherapy for unresectable sacral chordomas. Clin Cancer Res. 2004;10(17):5741–6.
5. Suzuki H, Yamashiro K, Takeda H, Nojima T, Usui M. Extra-axial soft tissue chordoma of wrist. Pathol Res Pract. 2011;207(5):327–31.
6. Nielsen GP, Mangham DC, Grimer RJ, Rosenberg AE. Chordoma peripheriсum: a case report. Am J Surg Pathol. 2001;25(2):263–7.
7. van Akkooi AC, van Geel AN, Bessems JH, den Bakker MA. Extra-axial chordoma. J Bone Joint Surg Br. 2006;88(9):1232–4.
8. DiFrancesco LM, Davanzo Castillo CA, Temple WJ. Extra-axial chordoma. Arch Pathol Lab Med. 2006;130(12):1871–4.
9. O'Donnell P, Tirabosco R, Vujovic S, et al. Diagnosing an extra-axial chordoma of the proximal tibia with the help of brachyury, a molecule required for notochordal differentiation. Skelet Radiol. 2007;36(1):59–65.
10. DeComas AM, Penfornis P, Harris MR, Meyer MS, Pochampally RR. Derivation and characterization of an extra-axial chordoma cell line (EACH-1) from a scapular tumor. J Bone Joint Surg Am. 2010;92(5):1231–40.
11. Lantos JE, Agaram NP, Healey JH, Hwang S. Recurrent skeletal extra-axial chordoma confirmed with brachyury: imaging features and review of the literature. Skelet Radiol. 2013;42(10):1451–9.

12. Rekhi B. Primary, large extra-axial chordoma in proximal tibia: a rare case report with literature review and diagnostic implications. APMIS. 2016;124(3):238–42.
13. Evans S, Khan Z, Jeys L, Grimer R. Extra-axial chordomas. Ann R Coll Surg Engl. 2016;98(5):324–8.
14. Robinson P, White LM, Sundaram M, et al. Periosteal chondroid tumors: radiologic evaluation with pathologic correlation. Am J Roentgenol. 2001;177:1183–8.
15. Nakatani T, Yamamoto T, Akisue T, et al. Periosteal osteoblastoma of the distal femur. Skelet Radiol. 2004;33:107–11.
16. Azouz EM, Saigal G, Rodriguez MM, Podda A. Langerhans cell histiocytosis: pathology, imaging and treatment of skeletal involvement. Pediatr Radiol. 2005;35:103–15.
17. Alberghini M, Pasquinelli G, Zanella L, et al. Primary malignant myoepithelioma of the distal femur. APMIS. 2007;115(4):376–80.
18. Lin CY, Kao CH, Liang JA, Hsieh TC, Yen KY, Sun SS. Chordoma detected on F-18 FDG PET. Clin Nucl Med. 2006;31(8):506–7.
19. Park SA, Kim HS. F-18 FDG PET/CT evaluation of sacrococcygeal chordoma. Clin Nucl Med. 2008;33(12):906–8.
20. Miyazawa N, Ishigame K, Kato S, Satoh Y, Shinohara T. Thoracic chordoma: review and role of FDG-PET. J Neurosurg Sci. 2008;52(4):117–21. discussion 121–2
21. Figl M, Leixnering M. Retrospective review of outcome after surgical treatment of enchondromas in the hand. Arch Orthop Trauma Surg. 2009;129(6):729–34.
22. Morris CJ, Younan Y, Singer AD, Johnson G, Chamieh J, Datir A. Masses of the hand and wrist, a pictorial review. Clin Imaging. 2016;40(4):650–65.
23. Athanasian EA. Bone and soft tissue tumors. In: Hotchkiss RN, Pederson WC, Wolfe SH, Kozen SH, editors. Green's operative hand surgery. 6th ed. Philadelphia: Elsevier Health; 2010.
24. Payne WT, Merrell G. Benign bony and soft tissue tumors of the hand. J Hand Surg Am. 2010;35(11):1901–10.
25. Henderson M, Neumeister MW, Bueno RA Jr. Hand tumors: II. Benign and malignant bone tumors of the hand. Plast Reconstr Surg. 2014;133(6):814e–21e.
26. Melamud K, Drapé JL, Hayashi D, Roemer FW, Zentner J, Guermazi A. Diagnostic imaging of benign and malignant osseous tumors of the fingers. Radiographics. 2014;34(7):1954–67.
27. Miller TT. Bone tumors and tumor like conditions: analysis with conventional radiography. Radiology. 2008;246(3):662–74.